ELSEVIER

Chemical Engineering Journal 131 (2007) 113–121

Chemical Engineering Journal

www.elsevier.com/locate/cej

A simplified chemical kinetics model for decomposition of Trigonox 21S

Bronislav V. Librovich [a,*], Andrzej F. Nowakowski [b], Andre Rovetta [c]

[a] *Naval Architecture and Marine Engineering, University of Strathclyde, Henry Dyer Building, 100 Montrose Street, Glasgow G4 0LZ, UK*
[b] *Department of Mechanical Engineering, University of Sheffield, Mappin Street, Sheffield S1 3JD, UK*
[c] *Sanofi Aventis Chimie Route D'Avignon, 30390 Aramon, France*

Received 15 June 2006; received in revised form 11 December 2006; accepted 18 December 2006

Abstract

An investigation of decomposition of Trigonox 21S in Shellsol T has been carried out using the proposed algorithm. A series of calorimetry experiments were performed, where temperature and pressure of the system were monitored. The numerical code has been developed using an annealing optimisation algorithm to find chemical kinetics and the solubility of carbon dioxide in the reacting solutions. The overall decomposition reaction can be represented by a first-order reaction mechanism with a chemical reaction rate approximated by an Arrhenius type expression with a pre-exponential factor of $4.300 \times 10^{13}\ s^{-1}$ and an activation energy 1.227×10^5 J/mol with heat of reaction 1.904×10^5 J/mol. Sensitivity analysis has been performed as well. It has been shown that the system is the most sensitive to the value of activation energy and logarithm of the pre-exponential factor.

Keywords: Trigonox 21S; Shellsol T; Decomposition; Chemical kinetics; PHI-TEC; Runaway reaction

1. Introduction

The knowledge of the chemical reaction kinetic in complex chemical systems is essential for the accurate and reliable design of reactors. It has a significant impact on the equipment needed in chemical production plants. The problem of an accurate design of chemical reactors is not only economical, it is directly related to safety issues and hazard assessment. Simplified or inaccurate design of a chemical reactor can lead to disastrous consequences. Without knowledge of chemical kinetic the chemical process can accelerate significantly and it can lead to runaway reaction and possible explosion of a reactor. For example, this was determined to be the course of the explosion on 8 April 1998 at Morton Chemical International (now Rohm & Haas) in Paterson, NJ, USA [1]. This reactor explosion had serious consequences, injuring nine people and two seriously. Hazardous materials were also released into the environment causing significant damage.

When chemical reactivity hazards are to be determined under a range of conditions, as for example with varying impurity levels, executing large or medium scale experiments is often impractical. Computer modelling of chemical kinetics based on data from smaller scale experiments provides a valuable information for simulating the system at larger scale, which otherwise could not be carried out experimentally due to environmental reasons.

The main problem in the modelling of complex kinetics is the huge amount of data needed to describe accurately the chemical processes. These data are not always available, and, even if they are known and accurate, in order to find important physical characteristics of a system extensive computational resources are required to perform numerical integration of a system of equations.

Usually, chemical process includes many, up to a several hundred, intermediate elementary reactions [2–4]. For example, in combustion science, it is very common to use complex multi-step reaction mechanisms to predict the oxidation of hydrocarbons [5,3].

In work by Tanaka et al. [3], a reduced kinetic model that included 32 species and 55 reactions was used to model homogeneous charge compression ignition in a rapid compression machine. This research shows that for heavy hydrocarbons, the ignition is a two stage process involving a low and high temperature stages. It has been shown that to model "knock" phenomena extensive chemical kinetic scheme is required. Oversimplified chemical kinetic scheme is unable to capture this well-known phenomena.

* Corresponding author.
E-mail address: bronislav.librovich@strath.ac.uk (B.V. Librovich).

1385-8947/$ – see front matter © 2007 Elsevier B.V. All rights reserved.
doi:10.1016/j.cej.2006.12.027

Nomenclature

A	empirical constant
B	empirical constant (K)
c	concentration (mol/m^3)
C	empirical constant (K)
C_p	heat capacity (J/(K kg))
E	activation energy (J/mol)
h	heat transfer coefficient (J/(m^2 K s))
H	enthalpy (J)
I	objective function
k	pre-exponential factor (s^{-1})
N	number of moles
p	pressure (Pa)
Q	external heat flux (J/s)
R	universal gas constant (J/(mol K))
S	surface area (m^2)
t	time (s)
T	temperature (K)
V	volume (m^3)
x	mole fraction in the liquid phase
y	mole fraction in the gas phase

Greek symbols

α	isobaric thermal expansivity (K^{-1})
ξ	extent of reaction (mol)

Subscripts and superscripts

c	calculated data
e	experimental data
g	gas
i	number of component
l	liquid
op	optimum value
r	reaction
s	surface
t	Trigonox
v	vapour
^	extensive value
-	intensive value

An extensive review of detailed chemical kinetic models for the combustion of hydrocarbon fuels has been written by Simmie [4], his review considered post-1994 work and was focused of the modelling of hydrocarbon oxidation in the gas phase by detailed chemical kinetics and those experiments which validate them.

Generic algorithm for optimisation of chemical kinetics reaction mechanism has been studied thoroughly in work by Elliott et al. [6]. The study has proved that generic algorithm can be used with much confidence to develop new, more effective reaction mechanisms for the combustion of complex hydrocarbon fuels by tuning the reaction rate coefficients.

A similar numerical analysis to the analysis used in the current paper was conducted to obtain the Arrhenius's type reaction rates for hydroxylammonium nitrate (NH_3OHNO_3) [7]. The reaction rates were obtained by an inverse analysis in a way that minimised an objective function, which was consisted of the difference between the calculated concentrations and experimental data as well as the uncertainties in the experimental data.

Table 1
Summary of the Trigonox decomposition experiments

Experiment	Trigonox (g)	Shellsol (g)	Initial temperature (°C)	Initial pressure (bar)
1	2.1	21.2	95.1	2.2
2	3.9	19.5	95.2	2.5
3	2.7	9.0	95.2	2.6
4	3.0	30.0	95.6	2.5
5	2.7	9.0	95.5	2.9
6	3.9	19.5	89.0	1.9
7*	2.7	9.0	94.9	1.5
8	2.7	9.0	95.1	1.7
9	1.9	9.6	84.7	2.1
10	2.0	9.5	95.1	1.5
11*	2.3	11.5	94.9	1.9

Due to complexity of the problem global chemical reaction scheme is widely used [8,9]. In some cases, the knowledge of complex chemical kinetics is not necessary, and using of global chemical kinetic scheme is sufficient and appropriate.

In this paper, the optimisation computer code has been developed and used to find the best chemical kinetics parameters for global scheme (Arrhenius's type) to fit data from the set of experiments in the most accurate way. The experiments for Trigonox decomposition were performed at Sanofi-Aventis, France.

2. Calorimetry experiments

A series of experiments on the decomposition of *tert*-butylperoxy-2-ethylhexanoate (Trigonox 21S)[1] were conducted. In these experiments, a varying mass of Trigonox was placed in a sealed PHI-TEC calorimeter (with a fixed volume of 59 ml) containing a varying mass of Shellsol T. Shellsol T is industrial solvent which is mixture of aliphatic hydrocarbons.[2] A summary of the masses used in the experiments is given in Table 1. The PHI-TEC calorimeter consists of a small thin walled test cell, of around 100 ml capacity, suspended in the centre of a set of electrically powered heaters within a stainless steel pressure vessel. The sample is placed in the test cell and heated until a substantial reaction rate is detected. At low temperature (∼20 °C) the decomposition rate of trigonox is low, and the period of half-decomposition can be up to several dozens days. The lack of strength of the thin walled test cells is compensated for by automatically applying an external nitrogen pressure. The cell contents may be stirred either magnetically or directly depending upon the type of test cell used.

In most of these experiments, the Trigonox was mixed with the Shellsol at low temperatures, and the mixture was heated to above the decomposition temperature of Trigonox. In the other experiments (which are marked with asterisk (*) in Table 1),

[1] Further this substance will be referred as Trigonox.
[2] Further this substance will be referred as Shellsol.

Table 2
Summary of the maximum temperatures and pressures and their time derivatives

Experiment	Maximum temperature, T_{max} (°C)	Maximum pressure, P_{max} (bar)	Maximum temperature derivative, $(dT/dt)_{max}$ (°C/s)	Maximum pressure derivative, $(dP/dt)_{max}$ (bar/s)
1	126.46	8.15	0.15	5.69×10^{-3}
2	154.80	16.10	0.37	0.14
3	174.63	13.57	2.20	2.63
4	122.37	10.37	0.11	4.32×10^{-3}
5	169.20	12.90	1.43	1.61
6	150.30	15.40	0.26	$9.55 \times ^{-2}$
7*	148.80	9.44	0.24	5.43×10^{-2}
8	173.26	14.08	1.90	3.21
9	150.26	8.62	14.86	5.59×10^{-2}
10	154.41	9.12	0.37	7.44×10^{-2}
11*	147.30	8.65	0.20	4.33×10^{-2}

the Shellsol was heated alone to above the decomposition temperature, and then the Trigonox was injected directly into the reactor. During the course of the runs, the temperature and pressure of the reactor together with the temperature of heating/cooling jacket were recorded. In Table 2, the maximum values of temperature, pressure, T_{max}, P_{max} and maximum values of their time derivatives $(dT/dt)_{max}$, $(dP/dt)_{max}$ are shown for all experiments.

If one assumes that all the carbon dioxide from the Trigonox decomposition is in the vapour phase and uses the ideal gas law to estimate the final pressure of the system, the resulting prediction would severely overestimate the pressure. This is due to the large solubility of carbon dioxide in the liquid phase.

3. Development of the mathematical model

3.1. Reaction kinetics

The reaction mechanism for the decomposition of Trigonox is quite complex and consequently, several species are evolved. The full reaction mechanism can contain dozens of elementary reactions. For industrial problems such kind of accuracy is not necessary, thus global scheme is commonly used. The global stoichiometric equation for Trigonox decomposition have the following form

$$\nu_t \underbrace{C_{12}H_{24}O_3}_{\text{Trigonox}} \Rightarrow \nu_{CO_2} CO_2 + \nu_h \underbrace{C_7H_{14}}_{\text{heptane}} + \nu_{t\text{-b}} \underbrace{C_4H_{10}O}_{t\text{-butanol}} + \text{other products.} \quad (1)$$

The stoichiometric coefficients are taken from experiment [10] and they are presented in Table 3. It is shown in table that the experimental stoichiometric coefficients of species below heptane are relatively small. To simplify the calculation and due to before mentioned fact these species are not included in the mathematical model. The stoichiometric coefficients for these species are zero in our model.

Although in this study the global stoichiometric equation is used, it will be shown further in the paper, that it is sufficient for prediction of system behaviour with sufficient accuracy required for industrial applications.

It is assumed that the reaction rate can be approximated by the relationship for the the first order reaction, where the kinetic rate is described using the Arrhenius's type relation

$$\frac{1}{V^l}\frac{d\xi}{dt} = k \exp\left(-\frac{E}{RT}\right) c_t, \quad (2)$$

where ξ is the extent of reaction (mol), V^l the total volume of the liquid phase, c_t the molar concentration of Trigonox in the liquid phase and k is a pre-exponential factor.

Table 3
Stoichiometric coefficients for the decomposition of Trigonox [10]

Species	ν_i	
	Experiment	Model
Trigonox	−1.00	−1.00
Carbon dioxide	0.80	0.80
t-Butanol	0.79	0.79
Heptane	0.65	0.65
t-Butyl-3-heptyl ether	0.13	0.00
C7–C15	0.14	0.00
C15 dimer	0.15	0.00
2-Ethylhexanoic acid	0.05	0.00
2-, 3-Heptane	0.04	0.00
Methane	0.02	0.00
Acetone	0.02	0.00

3.2. Species balance

Because the system is closed (i.e., no material can enter or leave the system), the balance equations for ith species is given by

$$\frac{dN_i^g}{dt} + \frac{dN_i^l}{dt} = \nu_i \frac{d\xi}{dt}, \quad (3)$$

where N_i^g and N_i^l are the total numbers of moles of component i in gas and liquid phases, respectively.

3.3. Energy balance

The increase of the total internal energy of the system is equal to the heat input (or output) by the surroundings

$$\frac{\mathrm{d}\hat{U}}{\mathrm{d}t} = Q. \tag{4}$$

It is assumed that the rate of heat transfer from the surroundings to the system is given by

$$Q = hS(T_\mathrm{s} - T), \tag{5}$$

where T is the temperature of the system, T_s the temperature of the heating/cooling jacket, h the heat transfer coefficient and S is the surface area for heat transfer to the calorimeter. The total internal energy of the system can be written as

$$\hat{U} = \hat{H} - p\hat{V} = \hat{H}^\mathrm{g} + \hat{H}^\mathrm{l} - p\hat{V}, \tag{6}$$

where $\hat{H}^\mathrm{g}$ is the total enthalpy of the vapour phase and $\hat{H}^\mathrm{l}$ is the total enthalpy of the liquid phase. Substituting this into the energy balance equation, the following is found

$$\frac{\mathrm{d}\hat{H}^\mathrm{g}}{\mathrm{d}t} + \frac{\mathrm{d}\hat{H}^\mathrm{l}}{\mathrm{d}t} - \frac{\mathrm{d}(p\hat{V})}{\mathrm{d}t} = Q \tag{7}$$

$$\frac{\mathrm{d}\hat{H}^\mathrm{g}}{\mathrm{d}t} + \frac{\mathrm{d}\hat{H}^\mathrm{l}}{\mathrm{d}t} - \hat{V}\frac{\mathrm{d}p}{\mathrm{d}t} = Q, \tag{8}$$

where the fact that the overall volume of the system remains constant have been used. Using the thermodynamic relation [11],

$$\mathrm{d}\hat{H} = \hat{C}_p\,\mathrm{d}T + \hat{V}\left[1 - \frac{T}{\hat{V}}\left(\frac{\partial\hat{V}}{\partial T}\right)_p\right]\mathrm{d}p + \sum_i \hat{H}_i\,\mathrm{d}N_i, \tag{9}$$

the following relation is obtained

$$\begin{aligned} Q = {} & (\hat{C}_p^\mathrm{g} + \hat{C}_p^\mathrm{l})\frac{\mathrm{d}T}{\mathrm{d}t} + \left\{\hat{V}^\mathrm{g}\left[1 - \frac{T}{\hat{V}^\mathrm{g}}\left(\frac{\partial\hat{V}^\mathrm{g}}{\partial T}\right)_p\right]\right. \\ & \left. + \hat{V}^\mathrm{l}\left[1 - \frac{T}{\hat{V}^\mathrm{l}}\left(\frac{\partial\hat{V}^\mathrm{l}}{\partial T}\right)_p\right]\right\}\frac{\mathrm{d}p}{\mathrm{d}t} + \sum_i \hat{H}_i^\mathrm{g}\frac{\mathrm{d}N_i^\mathrm{g}}{\mathrm{d}t} \\ & + \sum_i \hat{H}_i^\mathrm{l}\frac{\mathrm{d}N_i^\mathrm{l}}{\mathrm{d}t} - \hat{V}\frac{\mathrm{d}p}{\mathrm{d}t}, \end{aligned}$$

where $\hat{C}_p^\mathrm{g}$ is the overall heat capacity of the vapour phase, $\hat{C}_p^\mathrm{l}$ the overall heat capacity of the liquid phase, N_i^g the number of moles of ith species in the vapour phase, N_i^l the number of moles of ith species in the liquid phase, $\hat{H}_i^\mathrm{g}$ the partial molar enthalpy of ith species in the vapour phase and $\hat{H}_i^\mathrm{l}$ is the partial molar enthalpy of ith species in the liquid phase. Substituting the species balance equation yields

$$\begin{aligned} Q = {} & (\hat{C}_p^\mathrm{g} + \hat{C}_p^\mathrm{l})\frac{\mathrm{d}T}{\mathrm{d}t} + \left\{\hat{V}^\mathrm{g}\left[1 - \frac{T}{\hat{V}^\mathrm{g}}\left(\frac{\partial\hat{V}^\mathrm{g}}{\partial T}\right)_p\right]\right. \\ & \left. + \hat{V}^\mathrm{l}\left[1 - \frac{T}{\hat{V}^\mathrm{l}}\left(\frac{\partial\hat{V}^\mathrm{l}}{\partial T}\right)_p\right]\right\}\frac{\mathrm{d}p}{\mathrm{d}t} + \sum_i (\hat{H}_i^\mathrm{g} - \hat{H}_i^\mathrm{l})\frac{\mathrm{d}N_i^\mathrm{g}}{\mathrm{d}t} \\ & + \frac{\mathrm{d}\xi}{\mathrm{d}t}\sum_i \nu_i\hat{H}_i^\mathrm{l} - \hat{V}\frac{\mathrm{d}p}{\mathrm{d}t} \\ = {} & (\hat{C}_p^\mathrm{g} + \hat{C}_p^\mathrm{l})\frac{\mathrm{d}T}{\mathrm{d}t} + \left\{\hat{V}^\mathrm{g}\left[1 - \frac{T}{\hat{V}^\mathrm{g}}\left(\frac{\partial\hat{V}^\mathrm{g}}{\partial T}\right)_p\right]\right. \\ & \left. + \hat{V}^\mathrm{l}\left[1 - \frac{T}{\hat{V}^\mathrm{l}}\left(\frac{\partial\hat{V}^\mathrm{l}}{\partial T}\right)_p\right]\right\}\frac{\mathrm{d}p}{\mathrm{d}t} + \sum_i \Delta\bar{H}_i^\mathrm{v}\frac{\mathrm{d}N_i^\mathrm{g}}{\mathrm{d}t} \\ & + \frac{\mathrm{d}\xi}{\mathrm{d}t}\Delta H^\mathrm{r} - \hat{V}\frac{\mathrm{d}p}{\mathrm{d}t}, \end{aligned}$$

where the heat of reaction and the partial molar heat of vaporisation have been defined.

In order to simplify the model, it is assumed that the liquid phase behaves as an ideal solution and the vapour phase behaves as an ideal gas. In this case, for the vapour phase

$$p\hat{V}^\mathrm{g} = RT\sum_i N_i^\mathrm{g} \tag{10}$$

and

$$\hat{C}_p^\mathrm{g} = \sum_i N_i^\mathrm{g} C_{p,i}^\mathrm{g}, \tag{11}$$

where R is the universal gas constant and $C_{p,i}^\mathrm{g}$ is the molar heat capacity of species i in the gas phase. For the liquid phase

$$\hat{C}_p^\mathrm{l} = \sum_i N_i^\mathrm{l} C_{p,i}^\mathrm{l}, \tag{12}$$

where $C_{p,i}^\mathrm{l}$ is the molar heat capacity of pure liquid i. The total volume of the liquid phase $\hat{V}^\mathrm{l}$ is given by

$$\hat{V}^\mathrm{l} = \sum_i N_i^\mathrm{l}\bar{V}_i^\mathrm{l}, \tag{13}$$

where $\bar{V}_i^\mathrm{l}$ is the partial molar volume of species i in the liquid phase, which is assumed to be independent of composition. With these simplifications, it is found that

$$\begin{aligned} & \sum_i (N_i^\mathrm{g} C_{p,i}^\mathrm{g} + N_i^\mathrm{l} C_{p,i}^\mathrm{l})\frac{\mathrm{d}T}{\mathrm{d}t} + \hat{V}^\mathrm{l}\left(1 - \frac{\bar{V}_i^\mathrm{l}}{\hat{V}^\mathrm{l}}T\alpha_i\right)\frac{\mathrm{d}p}{\mathrm{d}t} + \sum_i \Delta\bar{H}_i^\mathrm{v}\frac{\mathrm{d}N_i^\mathrm{g}}{\mathrm{d}t} \\ & + \Delta H^\mathrm{r}\frac{\mathrm{d}\xi}{\mathrm{d}t} - \hat{V}\frac{\mathrm{d}p}{\mathrm{d}t} = Q, \end{aligned} \tag{14}$$

where

$$\alpha_i = \frac{1}{\bar{V}_i^\mathrm{l}}\left(\frac{\partial\bar{V}_i^\mathrm{l}}{\partial T}\right)_p \tag{15}$$

is the isobaric thermal expansivity of species i.

For condensible species, the heat of vaporisation was estimated using the Clausius–Clapeyron equation

$$\frac{\Delta \bar{H}_i^{\mathrm{v}}}{R} \approx \frac{\mathrm{d}\ \ln(p_i^{\mathrm{vap}})}{\mathrm{d}(1/T)} \approx \frac{1}{\log(\mathrm{e})} \frac{B_i}{(1 + C_i/T)^2}. \tag{16}$$

For non-condensible species (e.g., carbon dioxide), the heat of dissolution was estimated by

$$\frac{\Delta \bar{H}_i^{\mathrm{v}}}{R} = \frac{\mathrm{d}\ \ln H_i}{\mathrm{d}(1/T)} \approx -\frac{B_i}{\log(\mathrm{e})} \tag{17}$$

3.4. Volume equation

The total volume of the calorimeter remains constant, therefore, the following relation is satisfied.

$$\hat{V} = \sum_i N_i^{\mathrm{l}} \bar{V}_i^{\mathrm{l}} + \frac{RT}{p} \sum_i N_i^{\mathrm{g}}, \tag{18}$$

3.5. Phase equilibria

The conditions for phase equilibria between the vapour phase and the liquid phase must be satisfied. For gaseous species, the Henry's law is used

$$y_i p = H_i(T) x_i, \tag{19}$$

where $H_i(T)$ is the Henry's law constant, y_i the mole fraction of species i in the vapour phase and x_i is the mole fraction of species i in the liquid phase. The temperature dependence of the Henry's law constant is assumed to be given by

$$\log\ H_i(T) = A_i - \frac{B_i}{T}, \tag{20}$$

where A_i and B_i are material dependent empirical constants. For condensible species, the Raoult's law is used

$$y_i p = p_i^{\mathrm{v}}(T) x_i, \tag{21}$$

where $p_i^{\mathrm{v}}(T)$ is the vapour pressure of species i. The temperature dependence of the vapour pressure is given by Antoine's equation

$$\log\ p_i^{\mathrm{v}}(T) = A_i - \frac{B_i}{T + C_i}, \tag{22}$$

where A_i, B_i and C_i are material dependent empirical constants.

The accuracy of the proposed model can be improved in several ways. For example, the Peng–Robinson equation [12] may be used instead of equation for ideal gas, more sophisticated equation of state for liquid phase can be used, or Eq. (21) may be substituted by corresponding law with non-unity activity coefficients.

It is important to notice, that the most significant assumption is the fact that chemical kinetics of decomposition is approximated by global reaction rate (Eq. (2)). Thus, to improve accuracy of the model the previous assumption must be removed first, but, as it shown in the next section, even with this assumption the model describe the behaviour of the system with good accuracy.

Table 4
Parameters for the Henry's law constant "Eq. (20)" and the Antoine's equation "Eq. (22)"

Species	A_i	B_i	C_i
Trigonox	–	–	–
Carbon dioxide	To fit	To fit	–
t-Butanol	9.44484	1154.480	−95.500
Heptane	9.02023	1263.909	−56.718
Shellsol	9.71506	2009.16	−31.26

3.6. Parameter estimation

The values for various physical properties that were used in the model are summarised in Tables 4 and 5. Unless otherwise noted, the values are taken from [13,14]. In Table 4, the expression "to fit" denote the fact that these two parameters are determined from the optimisation algorithm.

4. Comparison of parameter fits with experiments

In each of the experiments, the temperature and pressure of the calorimeter contents were monitored. In addition, the temperatures of the heating/cooling elements, which were located at the top, side and bottom of the calorimeter, were also monitored. These temperatures varied with time and, in general, differed slightly from each other. In order to minimise the number of parameters in the model, the temperature of the heating/cooling jacket T_{s} of the calorimeter "see Eq. (5)" was taken to be the temperature of the side element.

For each experiment, the coupled differential–algebraic system which makes up the model, given by Eqs. (2)–(22) developed in the previous section, was numerically solved using DASPK subroutine libraries [15,16], which were integrated with the application code.

Table 5
Physical properties of various species

Species, i	Molecular weight (g/mol)	$C_{p,i}^{\mathrm{g}}$ (J/(mol K))	$C_{p,i}^{\mathrm{l}}$ (J/(mol K))	$\bar{V}_i^{\mathrm{l}}$ (cm^3/mol)	α_i ($\times 10^4$ K^{-1})
Trigonox	216.32	–	–	240.60	8
Carbon dioxide	44.01	37.13	–	–	–
t-Butanol	74.12	113.63	220.10	94.88	0
Heptane	100.20	165.20	224.98	147.47	0
Shellsol	172.00	–	344.	226.02	0
Nitrogen	28.97	29.08	–	–	–

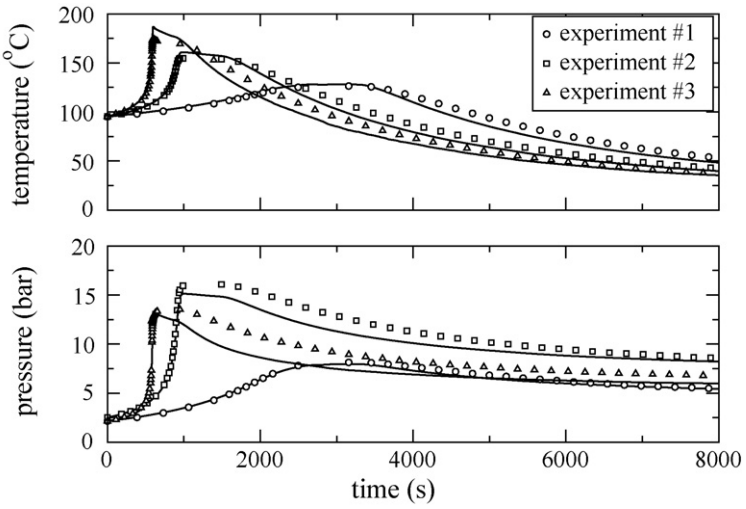

Fig. 1. Calculated and experimental temperature profiles for 1–3 experiments.

In order to solve an initial value problem for the derived differential–algebraic equation systems the equations were written in the general form

$$F\left(t, y, \frac{\mathrm{d}y}{\mathrm{d}t}\right) = 0, \tag{23}$$

where F, y and $\mathrm{d}y/\mathrm{d}t$ are N-dimensional vectors.

The variable step-size backward differential formula was used for an approximation of time derivatives. At each time step, the system of linear equations was solved by direct linear method.

The quality of the fit between the model with the experimental data was quantified by the following objective function:

$$I = \sum_{k=1}^{N} \left[\int_{t_{1,k}}^{t_{2,k}} \mathrm{d}t \left| \frac{T_k^{\mathrm{c}} - T_k^{\mathrm{e}}}{T_k^{\mathrm{e}}} \right| + \int_{t_{1,k}}^{t_{2,k}} \mathrm{d}t \left| \frac{p_k^{\mathrm{c}} - p_k^{\mathrm{e}}}{p_k^{\mathrm{e}}} \right| \right], \tag{24}$$

where N is the number of experiments (in our case $N = 11$) $t_{1,k}$ and $t_{2,k}$ times of the beginning and the end of kth experiment. Simulated annealing [17,18] was used to find the optimum values for model parameters (i.e., chemical kinetic constants, parameters for the Henry's law constant and total heat transfer coefficient, hS). A summary of the best fit parameter values are given in Table 6.

A comparison of the temperature and pressure profiles measured experimentally and calculated with the optimum model parameters, see Table 6, is presented in Fig. 1, for the first three initial experimental data sets. For all other initial experimental data comparison between measured and calculated data is good.

In all the experiments, similar behaviour of pressure and temperature is observed. Initially, the temperature is increasing due to release of thermal energy in chemical reaction, it reaches some maximum and later decrease due to heat losses into the cooling system. Thus, each experiment can be divided into two periods: chemical reaction and cooling periods.

In general, the agreement is good for the temperature profiles; the maximum deviation between the two is less than 8%. For pressure profiles, the difference between experimental and calculated data is larger and the maximum error is about 16%. Pressure profiles have similar tendency to temperature profiles.

From the results, the agreement between the best fit of the model and the experimental results worsens as the ratio of Trigonox to Shellsol increases. This trend is understandable, since the model describes the solubility of carbon dioxide in Shellsol using Henry's law. This is accurate, only when the predominant species in the liquid phase is Shellsol. As the ratio of Trigonox to Shellsol increases, the concentration of other species in the liquid phase, which are the decomposition products of Trigonox, increases and therefore, the accuracy of Henry's law is expected to diminish.

From these figures, it is possible to see that better agreement with experimental data takes place during chemical reaction period. From this fact, it is reasonable to conclude, that proposed global chemical kinetics scheme (2) describes well decomposition process.

In Fig. 2, calculated temporal dependence of mole number of different components in the gas phase are shown. For this figure initial values of the variables are taken from experiment number 1, see Table 1. The number of moles of carbon dioxide in the gas phase increase rapidly in the course of chemical reaction. Later, it decreases due to decrease of Henry's constant. The numbers of moles of reaction products t-butanol and heptane are also increasing during reaction period and decreases during cooling.

Table 6
Summary of best fit parameters for the reaction kinetics and Henry's law constants

Heat of reaction, H^{r} (J/mol)	Pre-exponent, k (s^{-1})	Activation energy, E (J/mol)	Henry's constant, $A_{\mathrm{CO_2}}$	Henry's constant, $B_{\mathrm{CO_2}}$ (K)
190,412.868	4.2996×10^{13}	122,658.016	8.3195	384.0196

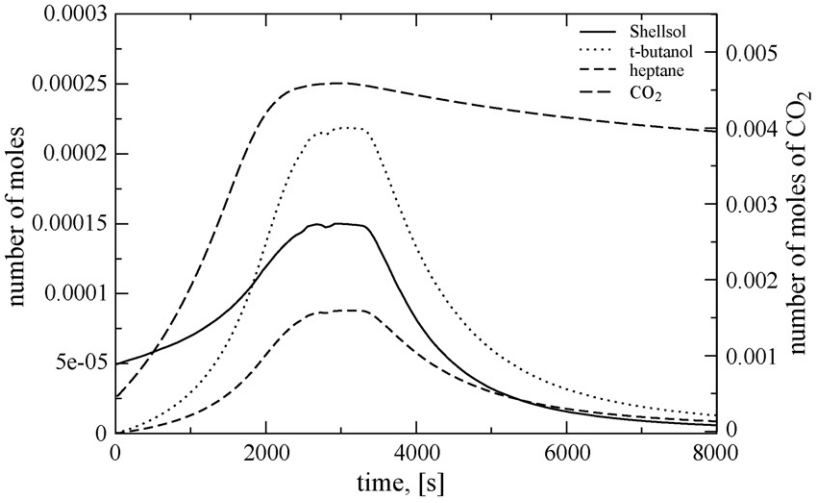

Fig. 2. Calculated profiles of number of moles in the gas phase, using optimum values of parameters and initial values from the experiment #1.

In Fig. 3, calculated temporal dependence of mole number of different components in the liquid phase together with chemical reaction rate are shown. In the liquid phase, the number of moles of Trigonox is decreasing monotonically due to chemical reaction, and on the contrary, the numbers of moles of reaction products are monotonically increasing. Chemical reaction rate has characteristic maximum. It increases initially due to temperature rising and decreases later due to consumption of Trigonox and temperature drop.

Fig. 4 represents Henry's law for CO_2 absorption in Shellsol together with other hydrocarbon liquids. As a comparison, we show the variation of the Henry's law constant with temperature for carbon dioxide in octane [19], decane [20], dodecane [21], hexadecane [22–28,20] and eicosane [29,27,30].

5. Sensitivity analysis

The obtained values of the parameters, see Table 6, require sensitivity analysis, in order to know how significantly the value of objective function will deviate from its minimum (optimum) value if the parameters will deviate from their optimum values. The sensitivity analysis was conducted in the following way. All parameters were kept fixed, apart from one, which varied in the interval $[0.95f_{k,\mathrm{op}}, 1.05f_{k,\mathrm{op}}]$, here $f_{k,\mathrm{op}}$ is the optimum value of kth parameter.

In Fig. 5, the dependence of non-dimensional objective functions, when all parameters are kept constant and equal to their optimum values apart from one, which was varied, are presented. As it is reasonable to assume, if the varied parameters were equal to the optimum value, $f_k/f_{k,\mathrm{op}} = 1$, then the non-dimensional objective function is equal to its minimum value, $I_k/I_{k,\mathrm{op}} = 1$. From this picture, it is easy to see that the system is more sensitive to the change of activation energy E and logarithm of the pre-exponential factor, $\ln(k)$. It is shown that if the activation energy changes on 5% ($f_E = 0.95f_{E,\mathrm{op}}$) the objective function increases on almost 250%, but if the heat transfer coefficient is changed by 5% ($f_h = 0.95f_{h,\mathrm{op}}$) the optimisation function is increased by less then 2%. Therefore, the small change in the

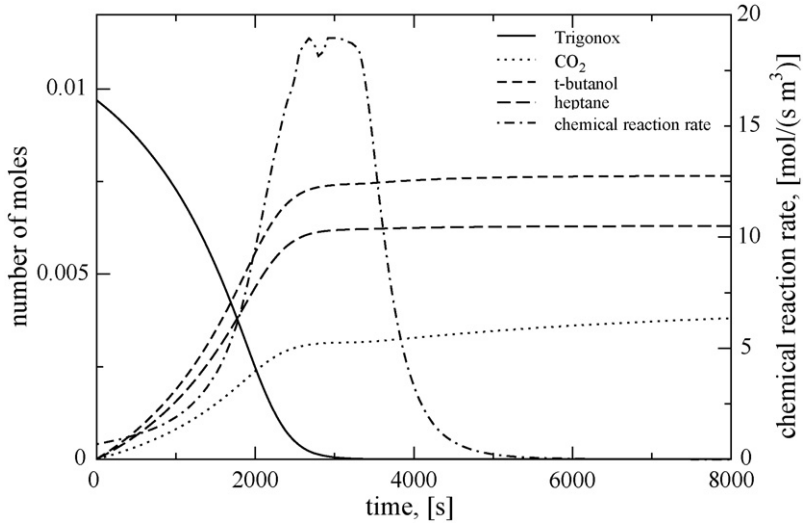

Fig. 3. Calculated profiles of number of moles in the liquid phase together with chemical reaction rate, using optimum values of parameters and initial values from the experiment #1.

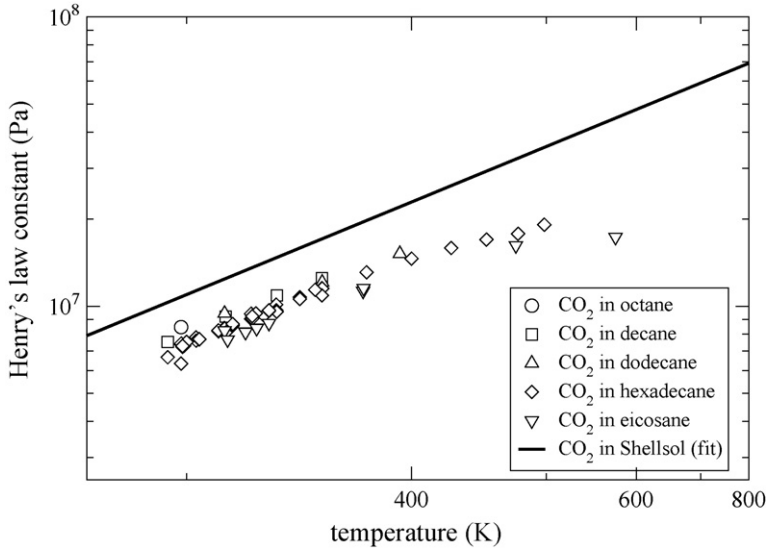

Fig. 4. Henry's law constant for the solubility of carbon dioxide in octane (circles), decane (squares), dodecane (triangles-up), hexadecane (diamonds) and eicosane (triangles-down). The solid line is the result of the parameter fit for the Henry's law constant of carbon dioxide in Shellsol.

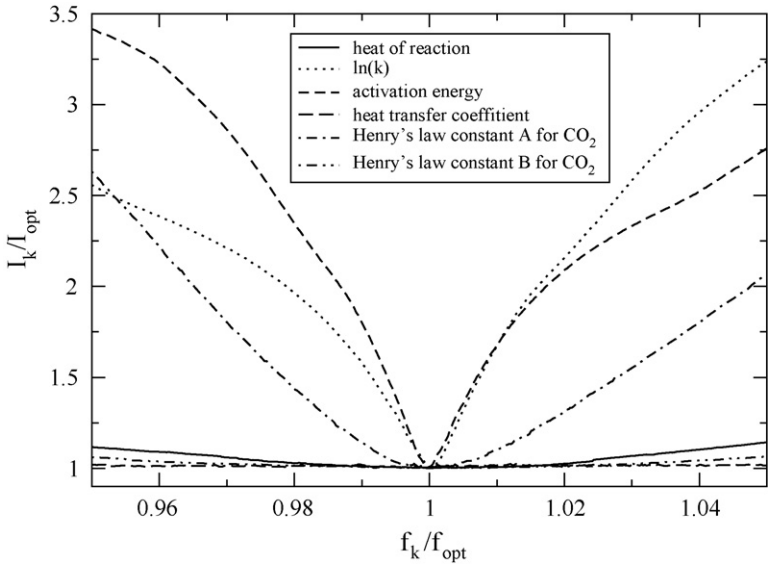

Fig. 5. Dimensionless optimisation function is presented as a function of several variable parameters. It has minimum value then varying parameter is equal to the optimum value.

activation energy or logarithm of the pre-exponent will lead to significant errors in calculations.

6. Conclusions

Experimental investigation of Trigonox decomposition in Shellsol have been performed. A numerical code has been written to solve the optimisation problem, in order to determine the optimum parameters. Although used for a specific set of experiments, the numerical study built up a general approach to generate parameters for the kinetic model. Using 11 experimental data sets (for pressure and temperature in the reactor together with heating/cooling jacket temperature) optimum parameters for global chemical kinetics scheme and Henry's law have been found. The maximum relative difference between calculated and experimental temperature profiles is about 8%, and for pressure profile is about 16%. Sensitivity analyses have been performed. It has been shown that the differential–algebraic system is most sensitive to two parameters, namely activation energy and logarithm of the pre-exponent. Calculated profiles of total number of moles of different species have been also presented together with the chemical reaction rate, which takes place in the liquid phase.

Acknowledgements

The authors acknowledge Dr. Leo Lue from the University of Manchester and Dr. Richard Rogers from Inburex GmbH, Germany, for their helpful suggestions and comments. The work was financially supported by the European Commission AWARD

project (Advanced Warning and Runaway Disposal, contract G1RD-CT-2001-00499) within the GROWTH program.

References

[1] Investigation Report: Chemical Manufacturing Incident, Technical Report, U.S. Chemical Safety and Hazard Investigation Board, 1998, http://www.csb.gov/completed_investigations/docs/MortonInvestigationReport.pdf.
[2] R. Vas Bhat, J. Kuipers, G. Versteeg, Mass transfer with complex chemical reaction in gas–liquid system: two-steps reversible reactions with unit stoichio-metric and kinetic orders, Chem. Eng. J. 76 (2000) 127–152.
[3] S. Tanaka, F. Ayala, J.C. Keck, A redused chemical kinetic model for HCCI combustion of primary reference fuels in a rapid compression machine, Combust. Flame 133 (2003) 467–481.
[4] J.M. Simmie, Detailed chemical kinetic models for the combustion of hydrocarbon fuels, Prog. Energy Combust. Sci. 29 (2003) 599–634.
[5] J. Warnatz, U. Maas, R. Dibble, Combustion: Physical and Chemical Fundamentals, Modeling and Simulation, Experiments, Polutant Formation, Springer-Verlag Berlin and Hiedelberg GmbH and Co. K, 2001.
[6] L. Elliott, D.B. Ingham, A.G. Kyne, N.S. Mera, M. Pourkashanian, C.W. Wilson, Generic algorithms for optimisation of chemical kinetics reaction mechanisms, Prog. Energy Combust. Sci. 30 (2004) 297–328.
[7] H. Lee, T.A. Litzinger, Chemical kinetic study of HAN decomposition, Combust. Flame 135 (2003) 151–169.
[8] H. Heinichen, A. Heyl, O. Rutsch, J. Weichmann, Modeling of the coplex chemical kinetics of the thermal decomposition of tetrachloromethane in methane, Chem. Eng. Sci. 56 (2001) 1381–1386.
[9] I.C. Rose, N. Epstein, A.P. Watkinson, Acid-catalyzed 2-furaldehyde (furfural) decomposition kinetics, Ind. Eng. Chem. Res. 39 (2000) 843–845.
[10] Mechanism for Thermal Decomposition of Trigonox 21S, Technical Report, Akzo Nobel Chemicals, 2004, http://www.akzonobel-polymerchemicals.com/.
[11] J.M. Smith, H.C.V. Ness, Introduction to Chemical Engineering Thermodynamics, McGraw-Hill, 1975.
[12] D.B. Robinson, D.Y. Peng, The Characterization of the Heptanes and Heavier Fractions for the GPA Peng–Robinson Programs, Technical Report, Gas Processors Association, Research Report RR-28, 1978.
[13] B.E. Poling, J.M. Prausnitz, J.P. O'Connell, The Properties of Gases and Liquids, McGraw-Hill, 2000.
[14] Shell Chemicals "Shellsol T", Technical Report, Shell, 2001, http://www.chembuyersguide.com/partners/shell.html.
[15] P.N. Brown, A.C. Hindmarsh, L.R. Petzold, Using Krylov method in the solution of large-scale differential–algebraic systems, SIAM J. Sci. Comp. 15 (1994) 1467–1488.
[16] P.N. Brown, A.C. Hindmarsh, L.R. Petzold, Consistent initial condition for differential–algebraic systems, SIAM J. Sci. Comp. 19 (1998) 1495–1512.
[17] A. Corana, M. Marchesi, C. Martini, Minimizing multimodal functions of continuous variables with the 'Simulated Annealing' algorithm, ACM Trans. Math. Softw. 13 (3) (1987) 262–280.
[18] W. Goffe, G. Ferrier, J. Rogers, Global optimization of statistical functions with simulated annealing, J. Econometrics 60 (1/2) (1994) 65–100.
[19] H. Josten, Separation of liquid mixtures by pressure of liquified gases, Ph.D. Thesis, RWTH Aachen, 1986.
[20] L. Zhang, S. Han, H. Knapp, Solubilities of carbon dioxide in mixtures of *n*-decane–*n*-hexadecane and *n*-heptane–toluene, Chin. J. Chem. Eng. 4 (2) (1996) 168–173.
[21] A. Henni, S. Jaffer, A.E. Mather, Solubility of N2O and CO2 in *n*-dodecane, Can. J. Chem. Eng. 74 (1996) 554–557.
[22] B.B. Breman, A.A.C.M. Beenackers, E.W.J. Rietjens, R.J.H. Stege, Gas–liquid solubilities of carbon dioxide, hydrogen, water, 1-alcohols ($1 \le n \le 6$), and *n*-parrafins ($2 \le n \le 6$) in hexadecane, octacosane, 1-hexadecanol, phen-athrene, and tetraethylene gycol at pressures up to 5.5 mPa and temperatures from 293 to 553 K, J. Chem. Eng. Data 39 (4) (1994) 647–866.
[23] M.K. Abu-Arabi, A.M. Al-Jarrah, M. El-Eideh, Physical solubility and diffusivity of CO_2 in aqueous diethanolamine solutions, J. Chem. Eng. Data 46 (3) (2001) 516–521.
[24] K.K. Tremper, J.M. Prausnitz, Solubility of inorganic gases in high-boiling hydrocarbon solvents, J. Chem. Eng. Data 21 (3) (1976) 295–299.
[25] P.J. Lin, J.F. Parcher, Direct gas chromatographic determination of the solubility of light gases in liquids, henry's law constants for eleven gases in *n*-hexadecane, *n*-octadecane, and *n*-hexatriacontane, J. Chromatogr. Sci. 20 (1982) 33–38.
[26] J.Y. Lenoir, P. Renault, H. Renon, Gas chromatographic determination of henry's constants of 12 gases in 19 solvents, J. Chem. Eng. Data 16 (3) (1971) 340–342.
[27] C.P. Chai, M.E. Paulaitis, Gas solubilities of CO_2 in heavy hydrocarbons, J. Chem. Eng. Data 26 (3) (1981) 277–279.
[28] G.H. Graaf, H.J. Smit, E.J. Stamhuis, A.C.M. Beenackers, Gas–liquid solubilities of the methanol synthesis components in various solvents, J. Chem. Eng. Data 37 (2) (1992) 146–158.
[29] K.A.M. Gasem, R.L. Robinson, Solubilities of carbon dioxide in heavy normal parraffins (C_{20}–C_{44}) at pressures to 9.6 mPa and temperatures from 323 to 423 K, J. Chem. Eng. Data 30 (1) (1985) 53–56.
[30] S.H. Huang, H.M. Lin, K.C. Chao, Solubility of carbon dioxide, methane, and ethane in *n*-eicosane, J. Chem. Eng. Data 33 (2) (1988) 145–147.